

Integration of Multi-source Data to Infer Effects of Gradual Natural Phenomena on Structures

Original

Integration of Multi-source Data to Infer Effects of Gradual Natural Phenomena on Structures / Lenticchia, Erica; Miraglia, Gaetano; Ceravolo, Rosario. - ELETTRONICO. - 270:(2022), pp. 572-581. (Intervento presentato al convegno European Workshop on Structural Health Monitoring EWSHM 2022) [10.1007/978-3-031-07322-9_58].

Availability:

This version is available at: 11583/2974131 since: 2023-01-12T19:01:12Z

Publisher:

Springer Nature

Published

DOI:10.1007/978-3-031-07322-9_58

Terms of use:

This article is made available under terms and conditions as specified in the corresponding bibliographic description in the repository

Publisher copyright

Springer postprint/Author's Accepted Manuscript (book chapters)

This is a post-peer-review, pre-copyedit version of a book chapter published in Lecture Notes in Civil Engineering. The final authenticated version is available online at: http://dx.doi.org/10.1007/978-3-031-07322-9_58

(Article begins on next page)

Integration of multi-source data to infer effects of gradual natural phenomena on structures

Erica Lenticchia ¹ [0000-0002-3746-2933], Gaetano Miraglia ¹ [0000-0002-3611-0215] and Rosario Ceravolo ¹ [0000-0001-5880-8457]

¹ Polytechnic of Turin, Turin 10129, Italy
erica.lenticchia@polito.it

Abstract. In Structural Health Monitoring for a real understanding of the changes taking place and their effects on the structural integrity of the built environment, sometimes it is necessary to move to long observation times. This follows the axioms of SHM, which identify a certain relationship between the frequency and time of observation and the extent (and therefore severity) of ongoing damage. For this reason, in the present paper, interferometric displacement satellite data acquired for a decade on the territory of the city of Rome (Italy) are investigated and correlated to natural phenomena. The paper critically analyzes the possibility of a relationship between these phenomena and satellite data in order to bring out a common pattern. The study of natural and anthropogenic phenomena in the same frequency bandwidth as the interferometric satellite data would therefore be useful for recognizing potential triggering causes of higher frequency phenomena, which could appear as sudden and unstable phenomena if observed with shorter times. In the paper, the authors first make a comparison between natural phenomena and satellite data on a territorial scale and then focus on a series of isolated case studies (single structures and infrastructures).

Keywords: First Remote Sensing, Satellite data; Structural Health Monitoring, Data Driven Approach, Interferometric Data, Architectural Heritage.

1 Introduction

As a result of natural instability phenomena (e.g., climate change) and anthropogenic interventions to transform the territory at a morphological and environmental level, calamitous events are becoming increasingly frequent and incisive in an already very fragile territory such as Italy.

Detecting and monitoring these phenomena and the possible disastrous consequence that they may have on the built environment is not a trivial matter. Although it is partially true that the increasing vulnerability may be due to the exceptionality of the event, on the other hand, inadequate or even lack of maintenance is usually the main cause. The need for a more effective safety assessment of strategic structures and infrastructures located in potentially sensitive areas, has pushed research to deepen the studies for the development of increasingly advanced techniques for structural health monitoring at different scales, from the territorial to the single building. In this regard, in recent years has received much attention the possibility of using data acquired from satellites to monitor physical phenomena at a territorial scale.

Satellite data have been used to monitor the effects of climate change, such as melting glaciers, fires, drought, and other phenomena; however, the potential of their employment for structural health monitoring (SHM) of the built environment is very recent [1]. Satellite data represent a promising source of information since interferometric data alone can detect centimetric even up to millimetric scale displacement. The first applications of satellite interferometric data concerned the monitoring of aggregated buildings in urban areas [2–4], the effects of land subsidence in built environments [5–7], and lately also applied to detect anomalies in single structures and infrastructures [8,9] recently has been published by the Italian consortium a first draft of the technical report on the [10].

Currently, the potentialities of these techniques appear to be of great interest, although the modalities of data processing and interpretation must necessarily be very different when passing from the territorial scale to that of the single structure or building. The combined use of multi-spectral satellite geophysical data with data acquired by continuous on-site measurements has been explored only by [11], and similar analyses of the combined use of on-site systems and remote acquisitions is a fundamental research theme that must be explored.

Despite the emerging literature, questions arise in the application of interferometric data to SHM in a broad sense. These data have been applied successfully to specific case studies; however, the result of the analyses are still case-by-case dependent since the same methodology cannot be applied with reliability to different case studies and always need manual adjustments and customization. In this paper, the authors want to explore what the satellite interferometric data can show if compared with some natural hazard phenomena and soil configuration, applying the study both to an urban area and localized structure. The aim is to analyze potential triggering causes of natural instability phenomena on building displacements and the correlation of these instabili-

ties with movements of structures observed by satellites. To this aim, a Geographical Information System (GIS) was aided with geologic cartography, natural hazards (such as landslides, sinkholes, etc.), and correlated with satellite interferometric data.

The paper is structured in three parts: (i) Section 2.1 explains the characteristics of selected case studies, which contemplate one urban area and one localized structure; (ii) Section 2.2 and Section 2.3 apply the comparative analysis between natural disaster, satellite data, and geological characteristics; finally, (iii) Section 3 reports conclusive discussion. This study is extremely important since the qualitative and quantitative assessment of buildings and infrastructures to such instability events could become a fundamental topic in developing policies and decisions on research, planning, prevention, and mitigation interventions.

2 Materials and method

Two main hazards have been considered for the urban analysis: landslides and sinkholes. The benchmark urban area was selected based on the built density and the presence of the specific geo-localized risk event. For the localized analysis, the structure of The Colosseum was chosen due to peculiar subsoil configurations.

2.1 Selected case studies

Historic Center of Central Archaeological Area. For this case study, priority was given to the number of events that occurred. In addition, the area has been experiencing an increase in the frequency of occurrence of these phenomena in recent years.

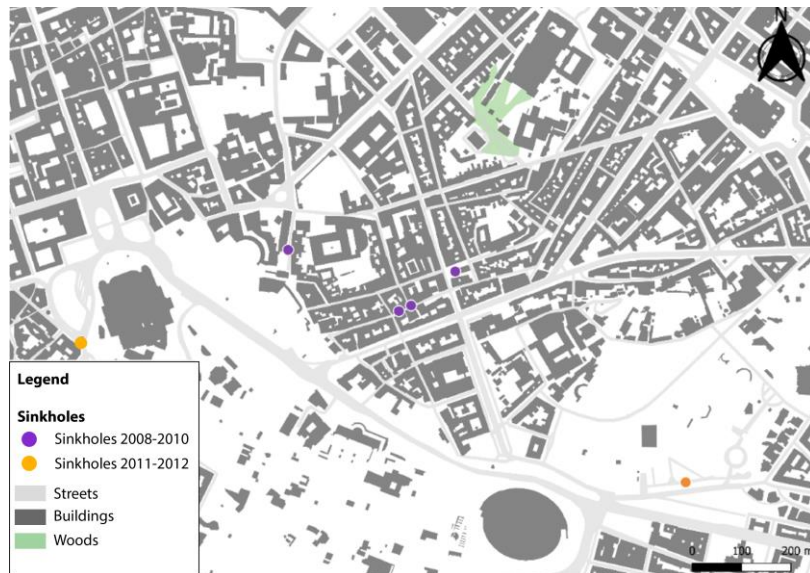


Fig. 1. Basic cartography of the Historic Center of Central Archaeological area.

It is located in the historic center of Rome, adjacent to the south of *Via Cavour* to the west of the *Altare della Patria* and *Fori Imperiali*, to the east of *Via del Boschetto*, and to the north of *Via Panisperna*. Four sinkholes occurred with a maximum distance of 250 m between 2011-2012; three of them occurred on the same day for the same reason: a violent storm. The sinkholes that occurred affected the roadways, damaging only the road surface and, in some cases, completely blocking the road system.

The area is predisposed to these types of phenomena because of the washout action in progress in the subsoil on materials with poor physical and mechanical characteristics [12]. Fig. 1 reports an essential cartography of the Historic Center of the Central Archaeological area.

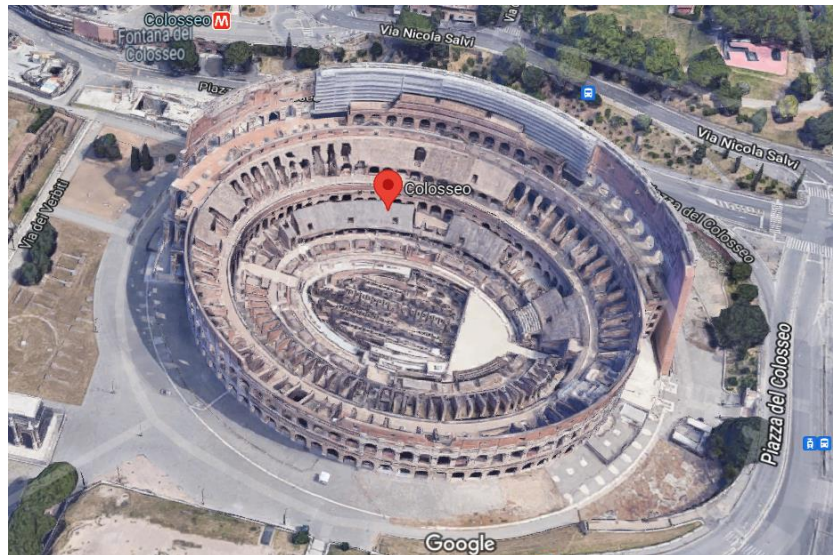


Fig. 2. Google Maps view of The Colosseum.

(<https://www.google.it/maps/place/Colosseo,+00184+Roma+RM/@41.8878913,12.4915933,390a,35y,39.36t/data=!3m1!1e3!4m5!3m4!1s0x132f61b6fc6433df:0x165f79d5d2332163!8m2!3d41.8905691!4d12.4922986> , on 01/02/2022 h. 16:31).

The Colosseum. The second case study regards the analysis of a large, monumental structure that is mainly distributed over a surface. The maximum plan dimensions of the Colosseum are approximately 188 m by 156 m, and the height of 48.5 m from the entrance level from the piazza. The great volumetric extension of the Colosseum could allow, in fact, to make initial comparative considerations with respect to the first two case studies; in particular, whether it is possible to capture and monitor soil-structure interaction phenomena due to differences in the conformation of the subsoil, thanks to interferometric data. The Colosseum presents a characteristic geological configuration, which has been thoroughly investigated by various studies [13]. In fact, the amphitheater site was originally an artificial lake placed along the course of the

Fosso Labicano. The Colosseum was built half on the bedrock, in this case consisting of conglomerates and sands pre-volcanic, and the other half on the talweg of *Fosso Labicano*. During the centuries, both the site and its surroundings had been modified: the artificial lake was filled, and the buildings surrounding the amphitheater were destroyed and rebuilt. As Cardarelli E. et al [14,15] point out, the site is subjected to specific geological conditions related to both natural geological factors as well as humanmade actions. Moreover, in recent years, this area has suffered numerous floods caused by extreme weather events and amplified by the topographical depression where the structure is located [16]. Such as the major flooding caused by the storm event on 20 October 2011, during which the underground structures (“hypogea”) were flooded by a copious amount of water that reached a depth of 6 m from the lowest level of the hypogea. Fig. 2 reports a view of The Colosseum.

2.2 Urban analyses: Historic Center of Central Archaeological Area

For urban analysis, the average annual trends of displacement, named *velocity*, v , in the paper, have been compared with geo-localized hazard events and geologic characteristics of the soil in the selected area. The velocity has been normalized in order to have a parameter, s , with values between 0 and 1 in the selected area, which simplify comparisons:

$$s = (v - |v|_{min}) / (|v|_{max} - |v|_{min}) \quad (1)$$

Then, several thresholds, $s_{thr}(n)$, of s have been analyzed based on the number, n , of standard deviations from the mean:

$$s_{thr} = |v|_{mean} \pm n |v|_{std} \quad (2)$$

Since negative values in v correspond to target points moving away from the satellite (e.g., subsidence), in the paper, the term *threshold* is referred to the bottom value of s_{thr} . In the analysis, n takes the values 1, 2, 3, 4, and 5.

The case study is characterized by a geological stratigraphy consisting of gravel, sand, clay, and several types of coastal tuff. In this area, three main zone worth of consideration can be underlined:

- Zone (a): This area starts from the *Altare della Patria* extending north/north-west over an area geologically characterized by a sandy and clayey gravel stratigraphy bordering a stratigraphic area of tuff located to the north-east. This cluster results to be the densest of points under the thresholds, characterized by historical building blocks with an average height of five-six floors and a heavy masonry structure.
- Zone (b): This area overlooks the Colosseum, along the via of *Fori Imperiali*, up to the intersection of *Via Cavour*, geologically characterized by tuff and sand that alternate with each other repeatedly. The area has a cluster of very numerous points below the threshold, which thin out along a line, in the areas of geological intercalation.
- Zone (c): Four sinkholes' events are geolocated in this zone. It is located north of *Via Cavour*, east of the *Fori Imperiali*, south of *Via Panisperna*,

and west of *Via del Boschetto*, in the historic center of Rome. Three of the four events took place in an area with lithological characteristics of gravel, sand, and clay, along *Via della Madonna dei Monti* and *Piazza della Madonna dei Monti*. The fourth event took place in an area with lithological characteristics of tuff, along the *Salita del Grillo*. Observing the cartography (see Fig. 3), in this zone, it can be seen that in the *Salita del Grillo*, there is the densest cluster of points below the threshold of the zone. This presence of points under the threshold thins out towards the Military Cathedral of Santa Caterina da Siena in Magnanapoli, where, since 2015, the presence of retrofitting structures of the external wall on the side of the *Salita del Grillo* has been detected.

In conclusion, as regards the geological characteristics and the points with subsidence below the threshold, also in this area, the phenomena already reported in the first case study are confirmed. It is worth noting that the only structure in which it is possible to verify the correspondence between points below the threshold and the presence of retrofitting interventions is the Church of Santa Caterina da Siena in Magnanapoli.

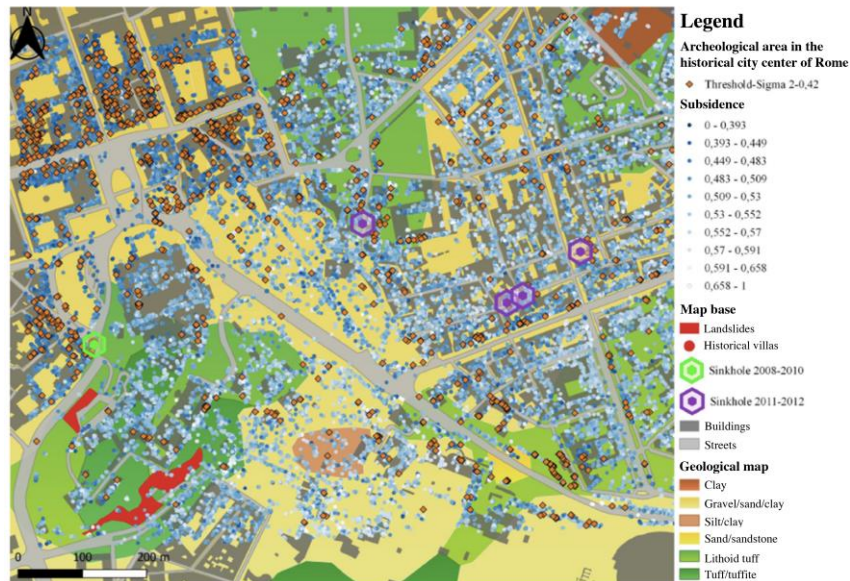


Fig. 3. Comparison between subsidence data (s parameter), hazard events, and geological characteristics of the Historic Center of Central Archaeological area: 2-sigma threshold ($n=2$).

2.3 Localized analysis: The Colosseum

For the localized analysis, in addition to the estimation of the normalized velocity, the points of The Colosseum were grouped in two zones: North and South (see Fig. 4 for clarity). The clusters reflect the actual configuration of the underlying soil. A Gaussi-

an distribution fitting was performed in each zone, highlighting potential differences. This was performed for both ascendent and descendent orbit data.

Fig. 4 and Fig. 5 report a map of the points observed by satellite that indicates the value of the normalized velocity over The Colosseum, and the Probability Density Functions (PDF) of velocity estimated for the two analyzed zones of the structure (i.e., North, and South zone, see Fig. 4), for ascendent orbit data. From Fig. 5, it is possible to observe a tendency of the structure to get close to the satellite, indicating a general upward movement rather than sinking. The upward trend movement is higher in the south zone, while remaining slower in the north (mean velocity of 0.0132 cm/year and 0.0215 cm/year in the north and south zones, respectively, with a difference of 0.0083 cm/year). It is worth noting that this is a general behavior of the structure as observed by ascendent orbit data, in fact, looking to the left tail of the distributions, it is possible to observe the presence with points at negative velocity, indicating that some points of The Colosseum are, actually, in a slow sinking, both in the North and South zone.

The same behavior, although confirmed, is not so markedly reflected in the data of the descending orbits, for which the mean velocity of the two zones is equal to 0.0175 cm/year and 0.0190 cm/year for the north and south zone respectively (with a difference of 0.0015 cm/year). The average velocity difference (evaluated with ascendent and descended orbit data) between the two zone results to be approximately ~ 0.0049 cm/year.

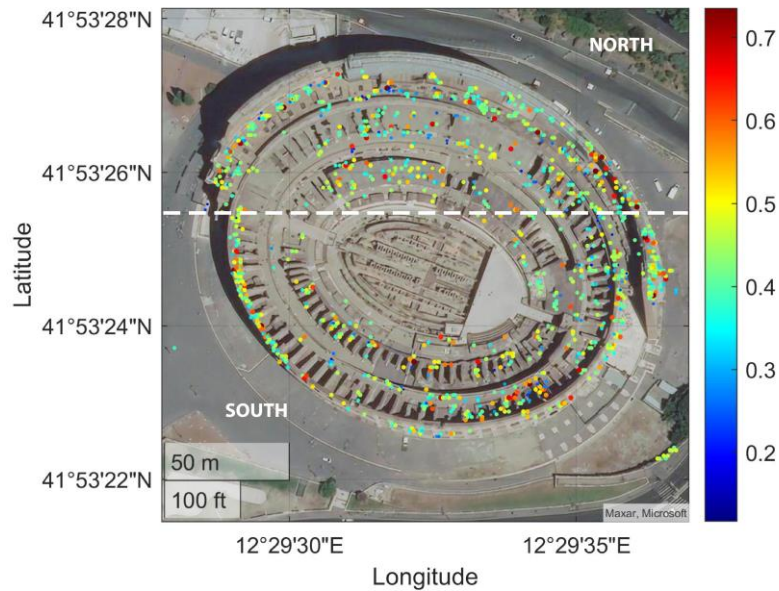


Fig. 4. Parameter s (i.e., normalized velocity) evaluated on the points of The Colosseum (ascendent orbit data).

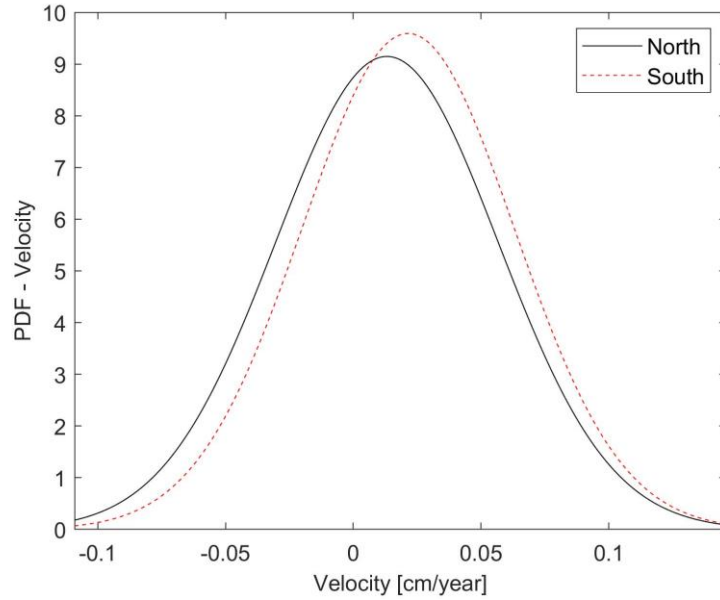


Fig. 5. Probability Density Function (PDF) of velocity, estimated with Gaussian distribution over the two zones (North and South, see Fig. 4) of The Colosseum (ascendent orbit data).

3 Results and Discussion

As regards the analysis on an urban scale, in the present study, it was possible to observe various correlations between the points with an average trend of displacement recorded by the satellite below the thresholds and the various hazard events. In particular, the correlation between the soil characteristics reported in the *Istituto Superiore per la Protezione e la Ricerca Ambientale* (ISPRA) geological map and the clusters of points below the threshold (characterized by high subsidence) was found. In the analyzed area, two main phenomena were detected: the first is (i) the high presence of points below the threshold in the territorial zones with different lithological structures, the second is (ii) the concentration of points with zero displacement trend in areas with geological characteristics of gravel, sand, clay, on which, among other things, large blocks of buildings and functional structures are concentrated.

Instead, for what concerns the localized analysis on the Colosseum, a slight difference was observed in the velocity data of the north and south areas; however, this almost imperceptible difference is difficult to interpret and could be due to, besides the different characteristics of the subsoil, also to uncertainties of observation and processing. This highlights how satellite data, if applied to urban scales, can find a more direct interpretation than that obtainable by applying them to single structures, for which further research is still necessary, as well as the need to integrate and

strengthen the considerations made using satellite data with reliable systems such as in situ testing and analysis.

As a future development, it would be interesting to observe a correlation between the flooding phenomena due to rainfalls and the points with subsidence values below the threshold to both scales of analysis.

References

1. Lenticchia, E.; Miraglia, G.; Ceravolo, R. Exploring Problems and Prospective of Satellite Interferometric Data for the Seismic Structural Health Monitoring of Existing Buildings and Architectural Heritage. In Proceedings of the 10th International Conference on Structural Health Monitoring of Intelligent Infrastructure; Porto, 2021.
2. Bonano, M.; Manunta, M.; Pepe, A.; Paglia, L.; Lanari, R. From previous C-band to new X-band SAR systems: Assessment of the DInSAR mapping improvement for deformation time-series retrieval in urban areas. *IEEE Trans. Geosci. Remote Sens.* **2013**, *51*, 1973–1984, doi:10.1109/TGRS.2012.2232933.
3. Cigna, F.; Lasaponara, R.; Masini, N.; Milillo, P.; Tapete, D. Persistent scatterer interferometry processing of COSMO-skymed stripmap HIMAGE time series to depict deformation of the historic centre of Rome, Italy. *Remote Sens.* **2014**, *6*, 12593–12618, doi:10.3390/rs61212593.
4. Zhu, M.; Wan, X.; Fei, B.; Qiao, Z.; Ge, C.; Minati, F.; Vecchioli, F.; Li, J.; Costantini, M. Detection of building and infrastructure instabilities by automatic spatiotemporal analysis of satellite SAR interferometry measurements. *Remote Sens.* **2018**, *10*, doi:10.3390/rs10111816.
5. Arangio, S.; Calò, F.; Di Mauro, M.; Bonano, M.; Marsella, M.; Manunta, M. An application of the SBAS-DInSAR technique for the assessment of structural damage in the city of Rome. *Struct. Infrastruct. Eng.* **2014**, *10*, 1469–1483, doi:10.1080/15732479.2013.833949.
6. Bozzano, F.; Esposito, C.; Mazzanti, P.; Patti, M.; Scancella, S. Imaging multi-age construction settlement behaviour by advanced SAR interferometry. *Remote Sens.* **2018**, *10*, doi:10.3390/rs10071137.
7. Ubertini, F.; Cavalagli, N.; Kita, A.; Comanducci, G. Assessment of a monumental masonry bell-tower after 2016 Central Italy seismic sequence by long-term SHM. *Bull. Earthq. Eng.* **2018**, *16*, 775–801.
8. Di Carlo, F.; Miano, A.; Giannetti, I.; Mele, A.; Bonano, M.; Lanari, R.; Meda, A.; Prota, A. On the integration of multi-temporal synthetic aperture radar interferometry products and historical surveys data for buildings structural monitoring. *J. Civ. Struct. Heal. Monit.* **2021**, *11*, 1429–1447.
9. Ponzio, F.C.; Iacovino, C.; Ditommaso, R.; Bonano, M.; Lanari, R.; Soldovieri, F.; Cuomo, V.; Bozzano, F.; Ciampi, P.; Rompato, M. Transport Infrastructure SHM Using Integrated SAR Data and On-Site Vibrational

- Acquisitions: "Ponte Della Musica--Armando Trovajoli" Case Study. *Appl. Sci.* **2021**, *11*, 6504.
10. Reluis Guidelines for the Use of Satellite Interferometric Data for the Interpretation of Structural Behavior of Constructions. *Tech. Guidel.* **2021**.
 11. Coccimiglio, S.; Coletta, G.; Lenticchia, E.; Miraglia, G.; Ceravolo, R. Combining satellite geophysical data with continuous on-site measurements for monitoring the dynamic parameters of civil structures. *Sci. Rep.* **2022**, *12*, 1–12.
 12. Ciotoli, G.; Corazza, A.; Finoia, M.G.; Nisio, S.; Serafini, R.; Succhiarelli, C. Sinkholes antropogenici nel territorio di Roma Capitale. *I Sink. Metodol. di indagine, Ric. Stor. Sist. di Monit. e Tec. di Interv. Centri abitati e Process. di Instab. Nat. valutazione, Control. e mitigazione. Mem. Descr. Cart. Geol. d'It* **2013**, *93*, 143–181.
 13. Funciello, R.; Lombardi, L.; Marra, F.; Parotto, M.; others Seismic damage and geological heterogeneity in Rome's Colosseum area: are they related? **1995**.
 14. Cardarelli, E.; Cercato, M.; Orlando, L. Geometry and seismic characterization of the subsoil below the Amphitheatrum Flavium, Rome. *Ann. Geophys.* **2017**, *60*, 436.
 15. Cavinato, G.P.; Moscatelli, M.; Stigliano, F.; Mancini, M.; Bianchi, L.; Cavuoto, G.; Cecili, A.; Cinnirella, A.; Corazza, A.; Di Luzio, E.; et al. Assetto geologico e idrogeologico del Colle Palatino--valutazione delle pericolosità geologiche. *Roma Archeol. Interv. per la tutela e la fruizione del Patrim. Archeol. Milan, Mondadori Electa, 1st Vol.* **2010**, 84–137.
 16. Di Salvo, C.; Mancini, M.; Cavinato, G.P.; Moscatelli, M.; Simionato, M.; Stigliano, F.; Rea, R.; Rodi, A. A 3D Geological Model as a Base for the Development of a Conceptual Groundwater Scheme in the Area of the Colosseum (Rome, Italy). *Geosciences* **2020**, *10*, 266.